Meandering rivulets on a plane : a simple balance between inertia and capillarity ?

Nolwenn LE GRAND-PITEIRA,* Adrian DAERR, and Laurent LIMAT
Laboratoire de Physique et Mécanique des Milieux Hétérogènes,
10 rue Vauquelin 75005 Paris France, UMR CNRS 7636
and Matière et Systèmes Complexes, University Paris 7, UMR CNRS 7057
(Dated: May 18, 2006)

Experiments on streams of water flowing down a rigid substrate have been performed for various plate inclinations and flow rates, and we focused on the regime of stationary meanders. The outcome is that (i) the flow is highly hysteretic : the shape of the meanders varies with flow rate only for increasing flow rates, and the straight rivulet regime does not appear for decreasing flow rate. (ii) A simple force balance, including inertia, capillary forces, and also hysteresis of wetting, accounts well for the experimental instability threshold flow rate and for the final radius of curvature of the meanders.

PACS numbers: 47.20.-k, 68.08.Bc, 47.60.+i, 47.20.Ma

Meandering is ubiquitous in nature and most familiar from rivers, but can also be seen at a much smaller scale like on window-panes during a rainfall. Recently, Drenckhan et al. [1] identified regular meandering patterns of rivulets, confined between two vertical plates, and charged with surfactants, mimicking undulations of foam Plateau borders. This observation confirms the generality of the pattern and suggests that a well defined mechanism is at work in rivulets, able to select a given meandering length scale. Understanding this mechanism and the properties of the resulting meanders is by itself a fundamental challenge which can also have implications in other fields of physics. For instance, Bruinsma [2] pointed out a possible analogy with the statistical mechanics for directed polymers inside a random matrix. The stability and characteristics of meandering rivulets may also be of importance to several industrial processes. In heat exchangers, changes between different flow regimes can cause drastic modifications of heat transfer [3]. Meander formation can also be an undesirable feature in coating processes [4].

For rivers [5, 6], it seems asserted that erosion is the key mechanism, but the meandering on non-erodible surfaces is still an essentially open problem. Culkin [7] and Nakagawa [8, 9] reported significant experimental work on streams running down an inclined plate. Nakagawa identified four regimes depending on flow rate : drops, meanders, unstable stream (the main rivulet oscillates and splits into several smaller ones) and a restable stream (the rivulet restabilizes into a straight rivulet of variable width, forming a braided pattern [10]). He stresses that he never obtained straight rivulets (of constant width), though this regime has been reported by Schmuki and Laso [11] who also investigated the effects of viscosity and surface tension, showing that meandering is suppressed at high viscosities. All in all, meandering has been observed in a wide variety of configurations, but little or no general conclusions have been drawn. In several studies the order parameter is the ratio of the length of the meanders over the length of the inclined plane (termed sinuosity, well kown in a geological context), a quantity difficult to interpret physically.

Stability analyses of rivulets, some neglecting longitudinal flow [12, 13], are mainly focused on varicose modes and not sinuous modes, i.e. are not dealing with the meandering instability. Only two recent papers deal with meandering threshold [2, 14].

This paper studies the shape and behavior of meandering rivulets as a function of two control parameters (flow rate and plate inclination), and discusses physical interpretations, focusing on the role of hysteresis. Up to now, there has been no quantitative study of the morphology of meanders on non-erodible surfaces in well controlled and reproducible conditions, and in addition, no comparison with simple hydrodynamic models. Our paper is a first step in this direction. In the present paper, experiments were only performed at low viscosity (that of water), corresponding to common natural situations.

Experimental set-up – Figure 1*a* shows a schematic diagram of the experimental set-up. De-ionized water is injected at the top of an inclined plate (1.20 m long and 50 cm wide). The substrate is a Mylar sheet (plastic sheets of polyethylene terephthalate (PET)), flattened on a rigid plate. It insures partial wetting conditions for wa-

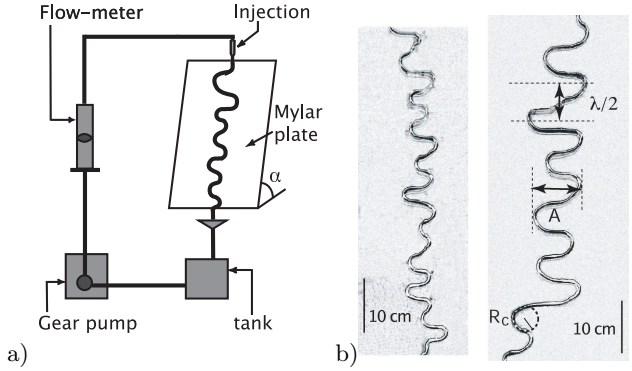

FIG. 1: a) Experimental setup b) Stationary meanders for $\alpha = 32°$. Q=1.08 mL/s for the left picture and Q=1.40 mL/s for the right one.

ter (advancing and receding contact angles of respectively $\theta_a = 70°$ and $\theta_r = 35°$) and reduces problems of static electricity compared to other common plastics. The tilt angle α of the plate can be changed at will between 0° and 87°. The water is collected in a tank and pumped back to the top of the plate by a gear pump providing an adjustable and constant flow rate Q, checked with a precision flow-meter. Pictures and movies of the experiments were taken by a digital camera placed 1 m above the plate and perpendicular to the latter.

Meandering thresholds – For increasing flow rates, the following regimes are observed. (i) Drops. Individual drops periodically detach from the injector [15]. (ii) Straight rivulets. The liquid flows down forming a straight continuous ridge along the direction of steepest descent. (iii) Meandering rivulets. Above a critical flow rate Q_{c1}, depending on the plate inclination, the straight stream is unstable. Perturbations (surface defects, injection noise, air movement, ...) appear as small bends of typical size comparable to the rivulet width w. These bends initially amplify laterally and downwards and eventually reach a stationary shape. It can take 10 minutes to one hour for a meander to fully develop along the whole length of the plate, but the resulting path is completely stationary (Fig. 1*b*). Snapshots of a settled meander, taken every 2 minutes during 24 hours, confirmed that it did not move at all throughout that time lapse. Using either a steady pump or a constant level tank, differently designed injectors and a long plate to check whether the behavior of the rivulet depended on the distance to the injector, we have verified that the meandering regime existed independently of injection conditions, confirming previous findings by other groups. To obtain yet other injection conditions, it might be interesting to study the collision/merging of two rivulets. (iv) Dynamic regime. Above a second critical flow rate Q_{c2}, meanders no longer remain stable. The rivulet sweeps from side to side, similar to the free end of a garden hose [16], frequently breaking up into sub-rivulets. (v) Restable regime. For even higher flow rates, the rivulet restabilizes and becomes straight again, but its width now varies like braids [10].

Fig. 2*a* displays the critical flow rates for the onset and disappearance of stationary meanders as a function of plate inclination α. The decrease of the second critical flow rate Q_{c2} with α is similar to that of Q_{c1}, but we have no explanation for it yet. The dependency of Q_{c1} on α can be understood from the balance of forces acting on the rivulet : gravity, surface tension, inertia and contact line pinning forces. For the lateral stability of a straight rivulet, gravity does not intervene (Fig. 2*b*). Surface tension opposes the bending of the rivulet and, once integrated across the cross-section, can be seen as a line tension of the liquid rim [17] creating a normal force F_γ straightening the rivulet. Taking into account the interfacial energies and the capillary pressure inside the rivulet, one gets $F_\gamma = C(\theta)\gamma w/r_c$, where $C(\theta)$ is a constant ($C(\theta) \approx \theta^2/3$ in the limit of a small average contact angle θ), γ the surface tension, w the width of the rivulet and r_c the initial radius of curvature. Pinning forces are reactive (therefore stabilizing forces) and act normal to the contact line. Their upper bound is given by the advancing and receding contact angles: $F_h \leq F_h^{\max} = \gamma(\cos\theta_r - \cos\theta_a)$. Instability will arise when inertia ($F_i = \rho S v^2/r_c$ where ρ stands for the density of the liquid, S for the cross-section of the rivulet and v for the RMS velocity ($\simeq$ average velocity) inside the rivulet) becomes stronger than both line tension and pinning ($F_i \geq F_\gamma + F_h^{\max}$). The onset of meandering is therefore given by:

$$\rho \frac{Q_{c1}^2}{S r_c} = \gamma \left[\frac{C(\theta) w}{r_c} + (\cos\theta_r - \cos\theta_a) \right] \qquad (1)$$

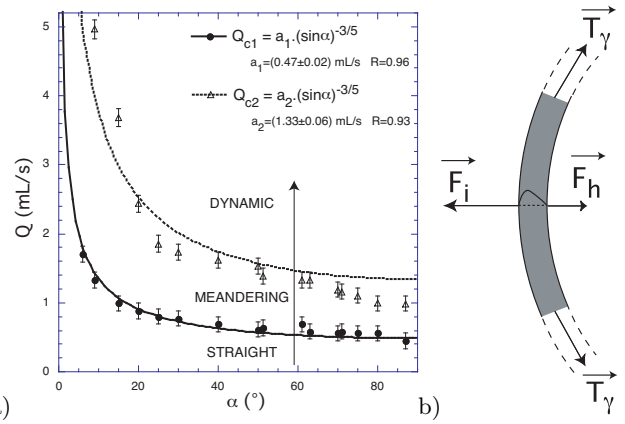

FIG. 2: a) Meandering thresholds for increasing flow rates b) Forces acting on a meander, in the plane of the plate

Without the pinning term, this balance was also suggested by Drenckhan *et al.* [1] for meanders in foams. If the pinning term can be neglected, or else if r_c scales as w with flow rate, the first critical flow rate scales as $\rho Q_{c1}^2/S \propto \gamma w$. Let us now assume that the flow inside the rivulet is a Poiseuille flow ($v \propto w^2 g \sin\alpha/\nu$), where ν denotes the kinematic viscosity), and approximate the cross-section of the rivulet to a disc segment with $\pi/4$ contact angle ($S = (\pi - 2)w^2/8$). Using flow rate conservation ($Q = Sv$) leads to the scaling

$$Q_{c1} \propto \left[(\gamma/\rho)^{4/5} (\nu/g)^{3/5} \right] . (\sin\alpha)^{-3/5}, \qquad (2)$$

This scaling matches the experimental data very well (Fig 2*a*). If we keep the theoretical prefactor evaluating to about 2.3, we obtain flow rates 5 times too small. Rough estimates of the force terms in equ (1), using experimental data for typical threshold conditions, show that pinning is not completely negligible [18]. We thus expect equ (2) to underestimate the threshold. It is satisfying that the order of magnitude of the forces, and their

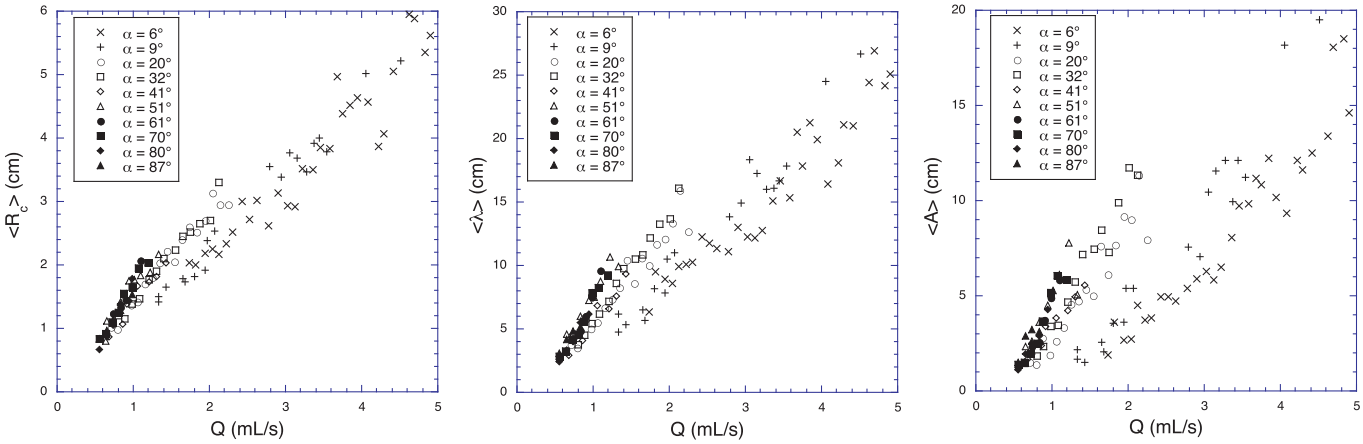

FIG. 3: Experimental data for the mean radius of curvature, wavelength and amplitude for numerous plate inclinations.

scaling, are correctly estimated. The scaling of equ (2) is close to that predicted by Bruinsma [2].

If the flow rate is now decreased while in the meandering regime, meanders remain remarkably stable: they keep their path, but become thinner, until they break up into drops. In particular there is no sinuous/straight rivulet transition: below Q_{c1} the rivulets meander instead of becoming straight. This strong hysteresis is a consequence of pinning effects. For all features of a meander with a radius of curvature greater than $C(\theta)w/(\cos\theta_r - \cos\theta_a) \approx 0.4w$, i.e. for all but very small scales, contact line pinning forces (now acting in the opposite direction) will dominate restoring capillary forces (equ. (1)), even if inertial forces tend to zero.

Shape of the stationary meanders – All the experimental data presented here were obtained for increasing flow rates. For numerous meanders achieved for plate inclinations varying between 6° and 87°, we measured the mean radius of curvature $\langle R_c \rangle$ at the apex of the curves (mean taken over all curves of a given rivulet), mean wavelength $\langle \lambda \rangle$, and mean amplitude $\langle A \rangle$ (see figures 1*b* and 3). All three parameters increase monotonically with the inclination of the plate α and the flow rate Q.

The magnitude of inertial and capillary forces depends on the shape of the rivulet path. The equilibrium of gravity, inertia, capillarity and pinning forces can therefore be used to solve for the expected radius of curvature of stationary meanders. Again, gravity does not matter if we are interested in the curvature at the vertical segments of the meander. The force balance at the threshold of depinning/motion then reads:

$$\left(\rho Q^2/S - C(\theta)\gamma w\right)/R_c = \gamma\left(\cos\theta_r - \cos\theta_a\right) \qquad (3)$$

This is the same as equation (1) except that R_c is now the final radius of curvature of the bends in the meander, which scales between 1 and 6 cm (see figure 3) and is much larger than the initial radius of curvature r_c considered for the threshold of the instability. An order of magnitude calculation [18] shows that the capillary contribution $C(\theta)\gamma w/R_c$ now becomes smaller than pinning,

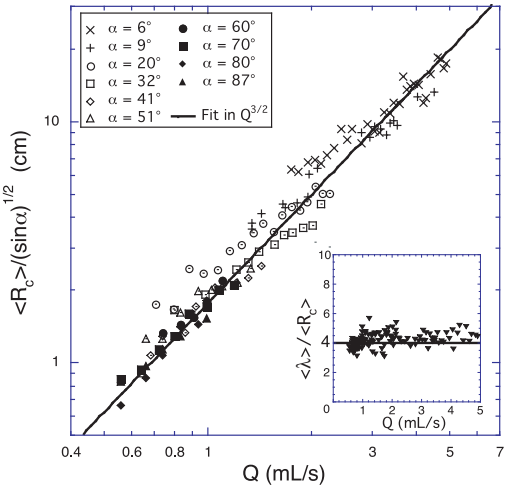

FIG. 4: Comparison of the data to the model for the mean radius of curvature. Insert: ratio of the wavelength to the radius of curvature for all plate inclinations α.

and is also smaller than inertia $\rho Q^2/(S.R_c)$. We therefore neglect the capillary part and, assuming a Poiseuille flow, one gets the following scaling law for the radius of curvature:

$$\langle R_c \rangle \propto \frac{\rho(g/\nu)^{1/2}}{\gamma(\cos\theta_r - \cos\theta_a)} Q^{3/2}\sqrt{\sin\alpha} \qquad (4)$$

This expression has been tested on our data (Fig. 4) and the scaling law fits the data reasonably well. The same scaling seems to hold for amplitude and wavelength.

Some sets of data, for a given inclination, seem to have a slightly different slope from the proposed scaling law. A first possible explanation lies in the neglected capillary term, which would add a contribution to the radius of curvature in $-Q^{1/4}\sin^{-1/4}\alpha$, which is more important at low inclinations and low flow rates, and diminishes the final radius. A second important point is the reduction of the effective slope through sinuosity $\mathcal{S}$(ratio of total length of the rivulet to the distance between its endpoints). The slope $\sin\alpha$ has to be replaced by $\sin\alpha/\mathcal{S}$ in equ (4), and since $\mathcal{S}$increases with Q and α [8], the

exponents of Q and α should be smaller than the ones in equ 4. Last not least, the Poiseuille flow assumption might need to be corrected. Indeed, flow visualizations with methylene blue dye show regions with zero or even backward recirculating flow, already mentioned by [19]. The Reynolds number based on the rivulet size is of order 500-1000.

Discussion – The scenario of development of meanders may be summed up as follows. Stable rivulets become unstable when inertia dominates capillary and pinning forces. The destabilizing term diminishes as a perturbation grows (and so its radius), so the hysteresis of wetting eventually stops the growth of the perturbation. In the final state, pinning forces should therefore be maximally mobilized, with the critical advancing contact angle on the outside of the curve and the critical receding contact angle on the inside. Cross-section measurements by Nakagawa and Scott [8] seem to corroborate this, but more quantitative measurements are planned.

As shown in fig 1*b*, the final meanders are made up of circular segments. The ratio $\langle\lambda\rangle/\langle R_c\rangle$ is expected to be close to 4 for paths made of half-circles possibly followed by horizontal segments. This is confirmed by the insert in fig 4 within experimental scatter.

In order to understand how the rivulet switches from one bend to the next, gravity has to be taken into account to explain why the rivulet does not follow the circular path back uphill. If weight is strong enough, it will exceed pinning at a critical orientation of the rivulet with respect to the slope, $\sin\Phi = \gamma(\cos\theta_r - \cos\theta_a)/\rho g S \sin\alpha$ which will define the inflection points on the path. If pinning always remains stronger, the rivulet can become horizontal without slipping : horizontal segments appear, in which the velocity decreases and the cross-section increases until gravity becomes dominant. Both scenari seem to correspond to observed patterns, but the effect on the amplitude of the meanders is not clear yet.

A last point remains to be discussed : above Q_{c1} perturbations are stabilized at large scales because the destabilizing forces decrease for smaller curvatures, but why do no new perturbations appear at small scales? A possible reason might lie in the considerable drop of the mean flow velocity (by more than a factor 2) at the transition from straight-to-meandering, which has been revealed by injection of methylene blue dye into the rivulets. The formation of a meandering path decreases the mean slope seen by the rivulet, and consequently the equilibrium velocity. The rivulet therefore becomes stable again in the meandering part, and remains unstable in the parts which have not yet developed bends. It would be interesting to perform velocity measurements to see whether the second threshold Q_{c2} is defined by the same critical local velocity as Q_{c1}.

Concerning the influence of viscosity on meanders, Schmuki and Laso [11] showed that viscosity damped meanders. Our scaling laws are in agreement with this observation : for higher viscosity, both the critical flow rate for the onset of meandering and the radius of curvature increase. Other experiments, varying viscosity, should be carried out to quantitatively determine the influence of viscosity on meandering.

Acknowledgments – We thank B. Andreotti and T. Podgorski for stimulating discussions and critical reading of the manuscript.

* Electronic address: nlegrand@pmmh.espci.fr

[1] W. Drenckhan, S. Gatz and D. Weaire, *Phys. Fluids*, **16**, 3115-3121 (2004)
[2] R. Bruinsma, *J. Phys. France*, **51**, 829-845 (1990).
[3] E. N. Ganic and M. N. Roppo, *ASME J. Heat Transf.*, **102**, 342-346 (1980)
[4] S. F. Kistler and P. M. Schweizer, Liquid film coating, edited by Chapmann & Hall (1997)
[5] L.B. Leopold and M.G. Wolman, *Bull. Goel. Soc. Am.*, **71**, 769-794 (1960)
[6] T.B. Liverpool and S.F. Edwards, *Phys. Rev. Lett.*, **75(16)**, 3016-3019 (1995)
[7] J. B. Culkin, *Ph. D. Northern University, Illinois*, (1982) ; J. B. Culkin and S.H. Davis, *AIChE Journal*, **30**, 263-267 (1984)
[8] T. Nakagawa and J. C. Scott, *J. Fluid Mech.*, **149**, 89-99 (1984)
[9] T. Nakagawa, *J. Multiphase Flow*, **18**, 455-463 (1992)
[10] K. Mertens et al, Nature 430 (2004) 165 and K. Mertens et al, J. Fluid. Mech. 531 (2005) 49
[11] P. Schmuki and M. Laso, *J. Fluid Mech.*, **215**, 125-143 (1990)
[12] S. H. Davis, *J. Fluid Mech.*, **98(2)**, 225-242 (1980) ; K. Sekimoto, R. Oguma and K. Kawazaki, *Ann. Phys.*, **176**, 359-392 (1987)
[13] G.W. Young and S.H. Davis, *J. Fluid Mech.*, **176**, 1-31 (1987) ; R.V. Roy and L.W. Schwartz, *J. Fluid. Mech.*, **391**, 293-318 (1999)
[14] H. Kim, J. Kim and B. Kang, *J. Fluid Mech.* **498**, 245-256 (2004)
[15] N. Le Grand, A. Daerr and L. Limat, *J. Fluid Mech.*, **541**, 293-315 (2005)
[16] S. Kuronuma and M. Sano, *J. Phys. Soc. Jpn*, **72**, 3106-3112 (2003)
[17] Two forces act normal on a meander section S : pressure $-S\Delta p$ and surface tension. The surface tension is made up of two parts : the water-air interface of length ℓ contributes a term $\gamma\ell$, the straight mylar-water interface of length w contributes a term $-\gamma w\cos\theta$ corresponding to the energy difference between wet and dry Mylar, θ being an average contact angle. The effective rivulet line tension is $T_\gamma = \gamma(\ell - w\cos\theta) - S\Delta p$. Approximating the water-air interface by a circular arc of radius r intersecting the solid plate at the contact angle θ, we find that $\ell = 2\theta r$, $w = 2r\sin\theta$, $\Delta p = \gamma/r$ (neglecting the longitudinal rivulet curvature) and $S = \theta r^2 - (1/2)wr\cos\theta$. The line tension becomes $T_\gamma = (1/2)\gamma w(\theta/\sin\theta - \cos\theta) = C(\theta)\gamma\omega$.
[18] For the contact angles given in the text, the pinning force is around $F_h = 35\,\mathrm{g.s^{-2}}$. Inertial and capillary terms evaluate to $\rho S v^2 = \rho Q^2/S = 50\,\mathrm{g.cm.s^{-1}}$ and $C\gamma w = 6\,\mathrm{g.cm.s^{-1}}$ for $Q = 1\,\mathrm{mL.s^{-1}}$, $w = 4\,\mathrm{mm}$.
[19] J. Walker, *Am. Sci.*, **253**, 132-137 (1985)